FINAL TECHNICAL REPORT

The BARD Continuous GPS Network: Monitoring Earthquake Hazards in Northern California and the San Francisco Bay Area, Collaborative Research between UC Berkeley and the USGS Menlo Park

Award Number:	G15AC00081
Start Date & End Date:	3/2015 – 3/2020
Principal Investigator:	Richard Allen, U.C. Berkeley
Email Address:	rallen@berkeley.edu
Co-Principal Investigator:	Noel Bartlow, U.C. Berkeley
Email Address:	nbartlow@berkeley.edu
Institution and Address:	University of California, Berkeley Berkeley Seismological Laboratory 215 McCone Hall # 4760 Berkeley, CA 94720-4760
Project Web Site:	http://seismo.berkeley.edu/bard

Acknowledgment of Support:
This material is based upon work supported by the U.S. Geological Survey under Grant No. G15AC00081.

Abstract

UC Berkeley's Seismological Laboratory (BSL) maintains the Bay Area Regional Deformation (BARD) network of permanent Global Navigation Satellite Systems (GNSS) stations to better understand crustal deformation in northern California and the timing and hazards posed by future earthquakes caused by strain accumulation along the San Andreas fault system in the San Francisco Bay area. BARD sites are also expected to be used for a geodetic component to the California earthquake early warning system, which is currently in development, and BARD sites will provide important displacement data and records of postseismic motion in the event of a large earthquake in Northern California. During this 5-year project period, we completed enhancements to the existing network including transitioning telemetry from frame relay to other options such as cellular modems or "host internet"; and upgrading most sites from GPS only to multi-constellation GNSS receivers. BARD data were used in a number of research projects; notably, real-time data streaming facilitated research into using these data for earthquake early warning applications. In particular, it facilitated the development of G-larmS, a geodetic-based earthquake early warning system that complements seismic-based warning systems by improving real-time magnitude estimates for very large earthquakes. G-larmS is currently undergoing

testing as part of the activities of the ShakeAlert Geodesy Algorithm Testing Implementation Subcommittee (GATIS).

1. Major Goals & Activities of the Geodetic Project

The Bay Area Regional Deformation (BARD) network is a collection of permanent, continuously operating Global Navigation Satellite System (GNSS) receivers that monitor crustal deformation in the San Francisco Bay Area (SFBA) and Northern California. Started in 1992 with two stations spanning the Hayward Fault, BARD has been a collaborative effort of the Berkeley Seismological Laboratory (BSL), the USGS, and several other academic, commercial, and governmental institutions. In the SFBA, nearly eight million people live in a geologically complex, tectonically active region that has experienced several historic earthquakes, including the 1868 Hayward, the 1906 San Francisco, and 1989 Loma Prieta earthquakes, and more recently the 2014 South Napa quake. In the 19th century alone, 16 M>6 earthquakes shook the region. Geologic, seismologic, and geodetic evidence suggest that the predominantly strike-slip deformation of the northwest-trending San Andreas fault system is an expression of the most active part of the boundary between the Pacific and North American plates.

The BARD network is designed to study the distribution of deformation in Northern California across the Pacific-North America plate boundary and interseismic strain accumulation along the San Andreas fault system in the Bay Area for seismic hazard assessment, and to monitor hazardous faults for emergency response. BARD sites are especially important for measuring interseismic strain accumulation due to their long period of operation, with most BARD sites predating other sites in the area by 5-10 years. In the event of a large earthquake, BARD sites will provide invaluable data for studying the earthquake rupture and postseismic slip. It also provides data in real-time for use in earthquake early warning (EEW) and rapid response applications. The BSL maintains and/or has direct continuous telemetry from 33 stations comprising the BARD Backbone, while additional stations operated by the USGS, US Coast Guard and others fill out the extended BARD network. BARD receivers originally used only the Global Position System (GPS) satellite constellation. Starting in 2018, BARD began the process of upgrading all receivers to multi-constellation GNSS receivers from Septentrio. Initial data from sites that have been upgraded show no detectable offset introduced by the receiver change, maintaining our continuous timeseries, along with a noticeable reduction in the time series noise.

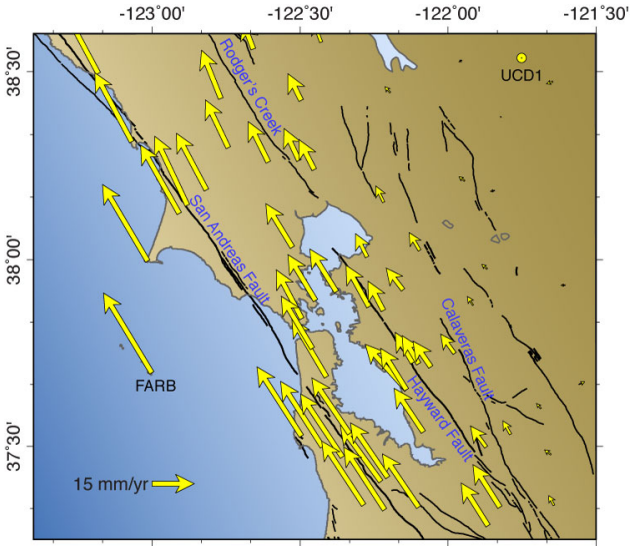

Figure 1: Interseismic velocities at BARD and PBO stations in the San Francisco Bay Area. Velocities are shown relative to site UCD1, located on the Sierra Nevada/Great Valley Block.

Since the completion of major construction on the Plate Boundary Observatory (PBO) portion of EarthScope in 2004, the number of GPS stations in Northern California has expanded

to over 250. Together, BARD, USGS, and PBO stations provide valuable information on the spatial complexity of deformation in the SFBA and Northern California, while the BARD network has the infrastructure and flexibility to additionally provide information on its temporal complexity over a wide range of time scales and in real-time. All BARD Backbone stations collect data at 1 Hz sampling frequency and stream their data in real-time to the BSL. These data are in turn provided in real-time to the public. Furthermore, eighteen BARD Backbone sites are co-located with broadband seismic stations of the BDSN, with which they share continuous telemetry to UC Berkeley.

Since its inception, BARD has been an important asset to the scientific community, supplying a core set of continuous sites which provide daily positions to track time dependent motion and a stable set of reference stations for campaign observations. Recent deformation modeling combing BARD data with other GPS sites and InSAR observations finds that deformation is mostly right-lateral strike-slip, distributed on multiple faults within the SFBA. The largest of these, the San Andreas Fault (SAF) accommodates 19 mm/yr or ~40% of the Pacific-North American relative plate motion, while the next largest Hayward fault accommodates 9.4 mm/year [*Xu, et al., 2018*]. Strain accumulation on the faults in the SFBA can be inferred from three-dimensional fault elastic dislocation modeling of the deformation field and is an important input in seismic hazard evaluations [e.g. *Bürgmann, Hilley, Ferretti, & Novali, 2006; Field et al., 2013; Field, et al., 2015; Zeng & Shen, 2016; Xu, et al., 2018*]. BARD sites are especially valuable for these studies.

The Working Group on California Earthquake Probabilities' UCERF3 report, which utilizes data from BARD stations, determines a 72% chance that a M 6.7+ earthquake will occur in the SFBA before 2045 including a 14.3% chance of a M 6.7+ earthquake on the Hayward fault specifically [*Field et al., 2015*]. The Hayward fault along the eastern side of San Francisco Bay is arguably one of the most hazardous faults in the world when one combines the probability of an earthquake with proximity to urban centers. The recent HayWired earthquake scenario estimates that for a magnitude 7.0 event on the Hayward fault, damages would total $82 billion, with an estimated 800 deaths and 18,000 non-fatal injuries [*Detweiler et al., 2017*]. BARD sites form an important part of the geodetic network near the Hayward fault, in particular sites SRB1 and MONB which are both very close to the fault. Historical accounts suggest that the northernmost Hayward fault has not ruptured for at least 170 or perhaps even 230 years [*Toppozada and Borchardt, 1998*], but geodetic data suggest that the northern Hayward fault is creeping within the seismogenic zone, potentially lowering the earthquake hazard [*Chaussard et al., 2015*]. However, dynamic weakening effects and the fact that the creep rate does not keep up with the full fault slip rate everywhere indicates that the Hayward fault may be a significant source of hazard. Additionally, geodetic data including data from BARD sites indicates that the southern Hayward and Calaveras faults are connected, indicating a previously unrecognized hazard that both may rupture together in earthquakes larger than magnitude 7 [*Chaussard et al., 2015*].

Geodetic measurements and modeling in the Bay area reveal a spatially complex deformation field with evidence for time-dependent strain that may affect the timing of future earthquakes. Postseismic transient deformation has been documented to occur for decades following the 1906 San Andreas earthquake [e.g. *Thatcher*, 1983] and for at least 25 years following the 1989 Loma Prieta earthquake [*Bürgmann et al.*, 1997; *Segall et al.*, 2000; *Huang et al.*, 2016]. This postseismic motion has been used to constrain the viscosity of the shallow crust and upper mantle in the region of the Loma Prieta earthquake [*Huang et al.*, 2016]. Stress changes from the

Loma Prieta earthquake also caused significant transient changes in shallow creep rates on the Hayward fault and the creeping SAF segment [*Lienkaemper et al.*, 1997; *Gwyther et al.*, 2000]. Stations from the BARD network are important sources of data for these studies and continued monitoring of postseismic transients on SFBA faults, especially given the long occupation time of most of our sites. Very recently, careful observations of decades-long GNSS time series near the Mendocino Triple Junction (MTJ) in Northern California including BARD sites YBHB and HOPB revealed sudden changes in velocity temporally co-incident with the timing of regional earthquakes with magnitude greater than 6.5. These velocity changes have been interpreted as previously unrecognized dynamically triggered changes in plate-interface coupling on the southern Cascadia subduction plate interface [*Materna et al.*, 2019].

Strain transients can also be self-nucleating, i.e. not triggered by an earthquake or other event. Slow slip events, with durations from hours to years, have been observed by GPS, strain- and creep-meters, in subduction zone regions and strike-slip environments [e.g. *Linde et al.*, 1996; *Miller et al.*, 2002]. Multiple slow earthquakes have also been observed on the SAF near San Juan Bautista. In 1992, a slip transient was detected over a 10-day interval on several borehole strainmeters, followed by events in 1996, 1998, 2002 and 2004 [*Linde et al.*, 1996; *Gwyther et al.*, 2000; *McFarland et al.*, 2013]. The 1998 transient event included aseismic slip both preceding and following an M5.1 earthquake on the SAF. This event was fortuitously captured by borehole strainmeters, creepmeters, BARD site SAOB, and a BDSN broadband seismometer [*Uhrhammer et al.*, 1999]. Slow slip events have also been detected using BARD and other GNSS sites in Parkfield [*Rousset et al*., 2018].

Slow slip events may occur wherever faults are creeping, this includes many faults throughout the Bay Area where they have not yet been observed. Triggered and spontaneous strain transients have been observed over a broad range of temporal scales and with over 20 years of operation, BARD network data is uniquely able to resolve past and longer-term slip-rate variations. The continued maintenance and operation of the BARD network will ensure that this long history of data collection continues into the future.

BARD sites have also contributed to studies of water storage in California, including drought monitoring and constraining the relationship between microseismicity and the seasonal hydrologic cycle [*Borsa et* al., 2014; Johnson *et al*., 2017].

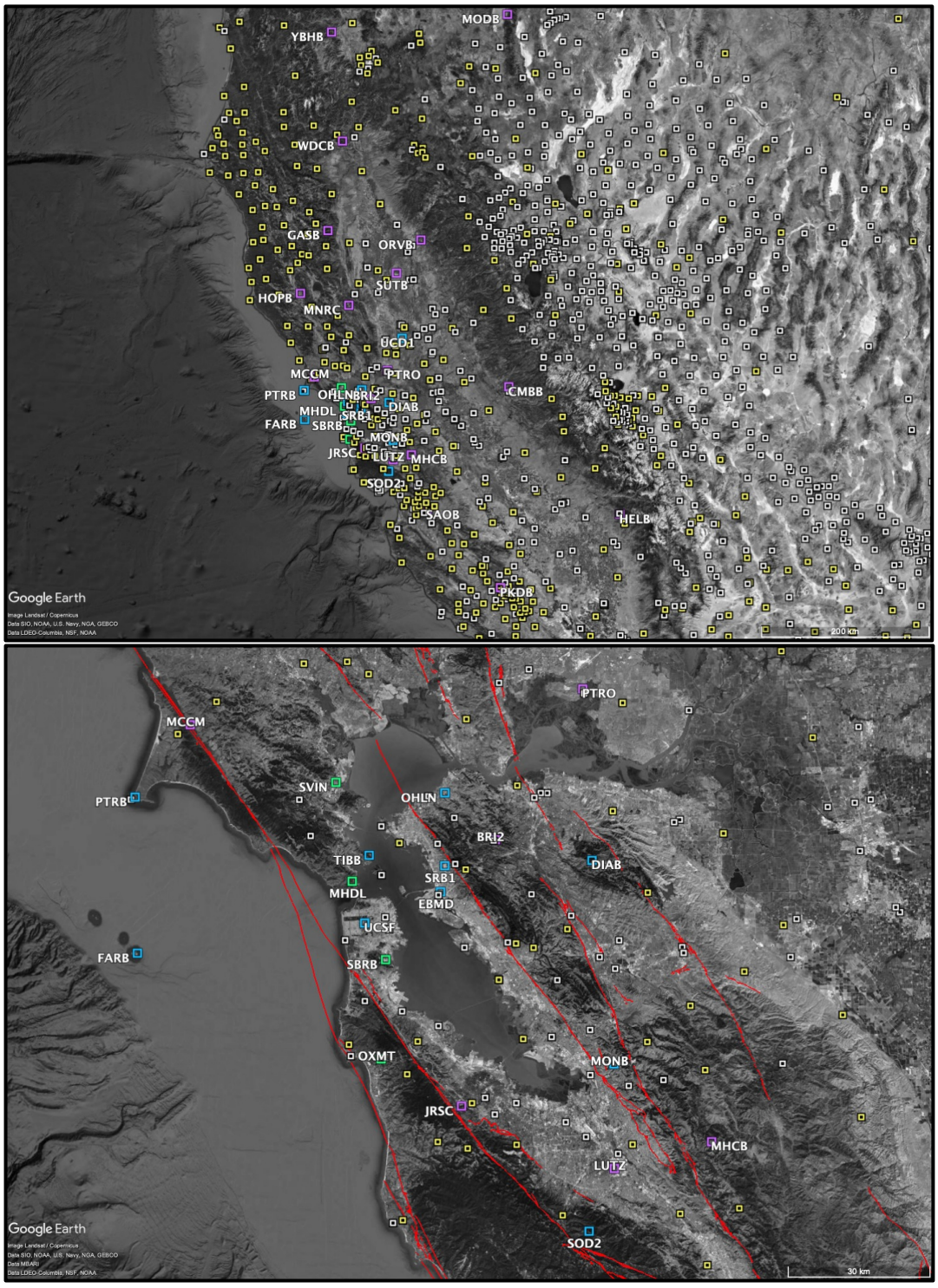

Figure 2: Map of the BARD network and surrounding GNSS sites in northern California. Labeled stations are part of the BARD network. Purple squares are BARD sites co-located with broadband seismic instruments; green squares are BARD sites co-located with borehole seismometers and 3-component strainmeters; yellow squares are Network of the Americas (NOTA) real-time sites; white squares are other GNSS sites. Top: Full network, Bottom: zoom in on the SFBA with major faults marked in red.

2. March 2015 - February 2020 Accomplishments

Supplement Funds to Renovate BRIB, SODB, PTRB and WDCB (2019-2020)
The monuments at several of the BARD GNSS stations were weakening, due to age or environmental influences, such as the near ocean environment. In particular, the metal supports for BRIB and SODB, two of our longest operating stations, and PTRB at Pt. Reyes National Seashore were rusting so badly that the antenna could move. In addition, the GNSS station at Whiskeytown National Recreation Area, WDCB, lost AC power in the Carr Fire in 2018 and went off-line when the batteries died shortly after the fire passed through its location. The BSL received supplement funds to renovate these station. Permitting for PTRB and WDCB has taken longer than expected; both are on lands managed by the National Park Service. We have been in discussions with the NPS staff at the two locations and hope to have a plan and permit in place to complete construction and upgrades later in 2020. Construction of new monuments and improvements to the infrastructure for the other two sites (SODB, now SOD2; BRIB, now BRI2) were completed in January 2020 and December 2019, respectively. Both sites now have Septentrio PolaRx5 receivers.

Station	*Land Host*	*Problems*	*Project Status*	*New Name*
BRIB	*UCB*	*Monument rusted/wiggly*	*Project completed Dec 2019. New monument constructed. Trimble NetRS receiver replaced by Septentrio PolaRx5 receiver.*	*BRI2*
SODB	*Private*	*Monument rusted/wiggly*	*Project completed Jan 2020. New monument constructed. Trimble NetRS receiver replaced by Septentrio PolaRx5 receiver.*	*SOD2*
PTRB	*NPS*	*Monument rusted/wiggly*	*In Dec 2019, the "monument" rusted out completely and broke off in a storm. All equipment and supplies to complete the project are "in hand". We are negotating with the Pt. Reyes National Seashore to complete the permit for the reconstruction.*	----
WDCB	*NPS*	*Damaged by Carr fire*	*WDCB sent data through the time the Carr Fire passed through the site, but the AC power failed. The SCIGN adapter partially melted. We had a site visit to evaluate replacing the equipment. Shortly after that visit, we were told by the NPS staff at Whiskeytown Recreation Area that they had bulldozed and removed everything associated with the station . All equipment and supplies to complete the project are "in hand". We are negotating with the Whiskeytown Rectreation Area to complete the permit for the reconstruction. The new site will have solar power.*	----

Field Installations and Testing of Septentrio PolaRx5 Receivers

Over the past 5 years, the BSL received funding to purchase 33 Septentrio PolaRx5 precise-point-position-capable receivers, enought to upgrade all the BARD GNSS stations it operates as well as the two contributing stations operated by partners. As of this report, twenty BARD sites so far have been upgraded with PolaRx5 receivers, including the two stations renovated with Supplement Funds. Sites with the new receivers show improvement in both the quality control data and the scatter in daily position timeseries (Figures 4 and 5). We expect to complete receiver upgrades at all BARD sites (pending permits for those still needing to be rebuilt, see report on Supplement Funds) by August 2020. Preparation to allow the installation of

the Septentrio PolaRx5 receivers included three important tasks, (a) testing the receivers with antennas from other manufacturers, (b) modifications to software to handle data from the receivers, and (c) preparing to configure the receivers for deployment.

(a) Testing Septentrio PolaRx5 Receivers: Before deciding, we tested the Septentrio PolaRx5 on the roof of McCone Hall. The goals of the test were to (i) study the quality of the onboard PPP engine which produces real-time positions and (ii) evaluate the performance of the sensor when used with different brands of chokering antennas. The latter is particurlarly important because the corrections necessary for PPP positioning are received by the GNSS antenna over L-band, so ascertaining whether different brands of chokering antennas have the bandwidth to receive the corrections is important. We found that the positions are of usually cm-level quality and that the L-band corrections are appropriately received with Ashtech, TopCon and Septentrio antennas. This is useful information because it means that the receivers can work in conjunction with any number of antennas.

(b) Software Modifications to handle data from the PolaRx5 receivers: The Septentrio PolaRx5 uses the open source BINEX format for storing data and transmitting data. However, because the units also calculate and provide PPP, they use an updated version of BINEX. Specifically, the PPP solutions are provided within a newly defined record within the BINEX format (record 0x05). Following the purchase of the PolaRx5, we had to update and test the acquisition software operating in the data center, so that it can handle and extract new BINEX records that are not present in data from our old Trimble and TopCon receivers. This work was done with advice and support from staff at UNAVCO and has recently been completed.

(c) Configuring Septentrio PolaRx5 receivers for field deployment: Mario Aranha spent significant time and effort developing procedures to properly set-up the Septentrio PolaRx5 receivers for field deployment. This involves direct coordination with Septentrio for each receiver deployment in order to properly configure the onboard PPP service. Mario's experience may be useful to the USGS or other organizations deploying these receivers.

Telemetry Replacement

Five years ago, many of the BARD sites were telemetered using the frame relay service from AT&T, which was deprecated in 2016/2017. During the project, all BARD sites were transitioned to other telemetry options, including "host internet", Uverse and cell modem, with the exception of GASB. That station had no options except satellite, although the equipment continues to run and we retrieve data via "sneakernet" when visiting the station. GASB is in a remote region of the Coast Ranges north of the Bay Area, where there is no cellular service.

Testing Trimble Kestrels at BRIB: During the first 2 years of the project, the company Trimble let us test the new, prototype "seismogeodetic" instrument, the Kestrel at the BARD site BRIB. The Kestrel is an instrument that combines geodetic and accelerometer data. Two test units were installed in September 2016. We chose this location as the T1 telemetry is not cost-limited and it is easy to access, being close to Berkeley. The Kestrels operated in parallel with the NetRS installed there, using data from the same GNSS antenna. Data from the GNSS part of the instrument were delivered to the datacenter in standard geodetic formats, while data from the accelerometer were delivered in a Trimble proprietary format and subsequently converted to EarthWorm. Finally, additional streams were also provided, such as precise point positioning (PPP) and acceleration-corrected displacement from the Kalman filtering of the PPP solutions

and the strong motion data (*Melgar et al*., 2013). We evaluated the data quality in order to determine the usefulness of this instrument for the long term mission of the network. While the data quality is acceptable, the processes for transmitting and receiving data, and for data retrieval do not fit well into the BSL's operations.

Deformation Monitoring:
In addition to the operation of BARD, this Cooperative Agreement funded the operation and maintenance of the deformation monitoring equipment at the sites BRIB, MHDL, OHLN, OXMT, SBRN and SVIN. Telemetry for these stations was also transitioned away from frame relay. BRIB (now BRI2) is on a T1 line operated by the Astronomy Department of UCB and MHDL is served by a Wireless Internet Service Provider (WISP). OHLN uses AT&T Uverse, and the other stations transmit over cell modem. Sadly, the tank at BRIB was flooded several times, most recently the winter 2016/2017. At this site, the BSL operates broadband and strong motion sensors and data loggers in addition to the downhole geophones, accelerometers and dilatometer. Electromagnetic sensors and data loggers that are part of a Stanford/USGS joint project are also installed at the site. We pumped most of the water out of the tank the first time, and retrieving the myriad data loggers, power support equipment and accelerometer. Rather than reinstall the equipment in the same tank and experiencing flooding again, we explored options for above-ground deployment of the equipment. Unfortunately, the current solution (moving the seismic station) does not include a way to collect data from the borehole sensors and dilatometer. We are still considering options for the deformation equipment at BRIB. In the meantime, the field team continues to support and make repairs at the other deformation sites.

Figure 4: Quality Control measurements for BRIB before and after the receiver change. MP1 and MP2 are measures of the RMS of the multipath part of the pseudorange. Completeness improved, multipath noise decreased, and signal-to-noise increased after the receiver upgrade on 09/01/2018 (vertical red line).

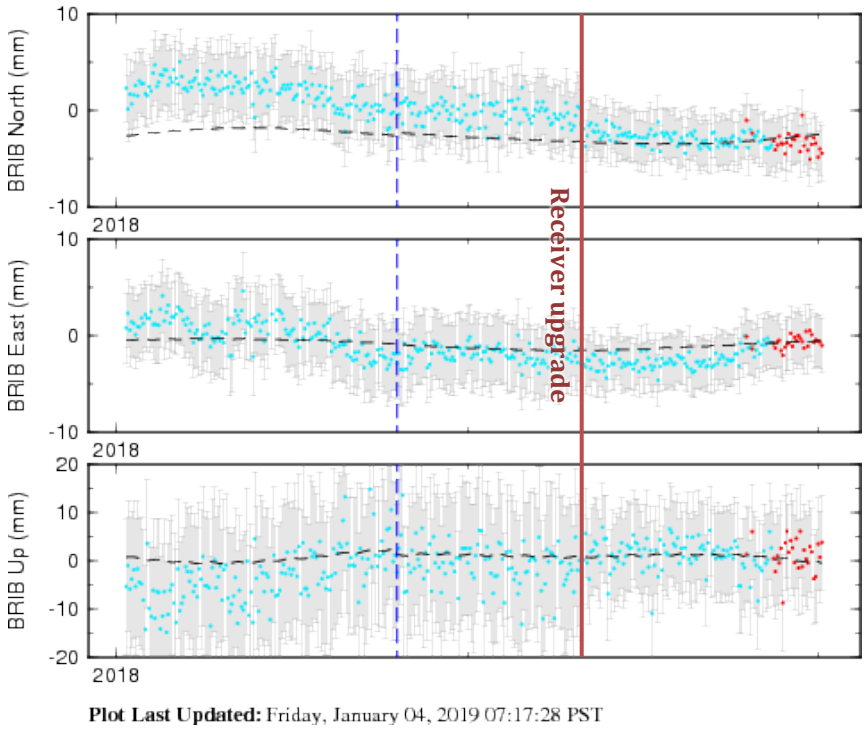

Figure 5: Daily position timeseries for BRIB provided by USGS for the one year. Note that at the time of the receiver upgrade the scatter and the estimated uncertainties decrease in all 3 components. No offset is observed at the time of the receiver upgrade.

2.1 *Station Upgrades and Current Configuration*

	Site	Lat. (deg)	Lon. (deg)	Receiver	Ant.	Telem.	Co-loc. Network	*Location*
1	BRI2	37.92	-122.15	PolaRx5	CR	T1	BDSN	*Briones Reservation*
2	CMBB	38.03	-120.39	NET-G3A	CR	Int	BDSN	*Columbia College*
3	DIAB	37.88	-121.92	PolaRx5	CR	CM		*Mt. Diablo*
4	FARB	37.70	-123.00	PolaRx5	CR	R-Int	BDSN	*Farallon Island*
5	GASB	39.65	-122.72	NET-G3A	CR		BDSN	*Alder Springs*
6	HELB	36.68	-119.02	PolaRx5	CR	R-CM	BDSN	*Miramonte*
7	HOPB	39.00	-123.07	PolaRx5	CR	CM	BDSN	*Hopland Field Station*
8	JRSC	37.41	-122.23	PolaRx5	CR	Int	BDSN	*Jasper Ridge Biological Preserve*
9	LUTZ	37.29	-121.87	PolaRx5	CR	Int	BDSN	*SCC Communications*
10	MCCM	38.14	-122.88	PolaRx5	CR	CM	BDSN	*Marconi Conference Center*
11	MHCB	37.34	-121.64	PolaRx5	CR	Int	BDSN	*Lick Observatory*
12	MHDL	37.84	-122.49	PolaRx5	CR	Int	Mini-PBO	*Marin Headlands*
13	MNRC	38.88	-122.44	NET-G3A	CR	VSAT	BDSN	*McLaughlin Mine*
14	MODB	41.90	-120.30	PolaRx5	CR	VSAT	BDSN	*Modoc Plateau*
15	MONB	37.49	-121.87	NET-G3A	CR	CM		*Monument Peak*
16	OHLN	38.01	-122.27	NET-G3A	CR	CM	Mini-PBO	*Ohlone Park*

	Site	Lat. (deg)	Lon. (deg)	Receiver	Ant.	Telem.	Co-loc. Network	*Location*
17	ORVB	39.55	-121.50	NET-G3A	CR	CM	BDSN	*Oroville*
18	OXMT	37.50	-122.42	NET-G3A	CR	CM	Mini-PBO	*Ox Mountain*
19	PKDB	35.95	-120.54	NETRS	CR	R-T1	BDSN	*Bear Valley Ranch*
20	PTRB	38.00	-123.01	NETRS	CR	R-Int		*Point Reyes Lighthouse*
21	PTRO	38.21	-121.94	NET-G3A	CR	CM	BDSN	*Potrero Hills*
22	SAOB	36.77	-121.45	NETRS	CR	CM	BDSN	*San Andreas Observatory*
23	SBRB	37.69	-122.41	PolaRx5	CR	CM	Mini-PBO	*San Bruno Replacement*
24	SOD2	37.17	-121.93	PolaRx5	CR	R-Int		*Soda Springs*
25	SRB1	37.87	-122.27	PolaRx5	CR	Fiber		*Seismic Replacement Building*
26	SUTB	39.21	-121.82	NETRS	CR	R-CM	BDSN	*Sutter Buttes*
27	SVIN	38.03	-122.53	PolaRx5	CR	R-CM	Mini-PBO	*St Vincents*
28	TIBB	37.89	-122.45	PolaRx5	CR	R-Int		*Tiburon*
29	UCSF	37.76	-122.46	PolaRx5	CR	Int		*UC San Francisco*
30	WDCB	40.58	-122.54	*Not operational*			BDSN	*Whiskeytown Dam*
31	YBHB	41.73	-122.71	PolaRx5	CR	CM	BDSN	*Yreka Blue Horn Mine*
Partner-operated BARD sites								
32	EBMD	37.82	-122.28	PolaRx5	CR	Int		*East Bay Mud Headquarters (Operated by EBMUD)*
33	UCD1	38.54	-121.75	PolaRx5	CR	Int		*UC Davis (Operated by UC Davis)*

Table 1. BARD station information with equipment and telemetry types to be maintained. Receivers are: Septentrio Polarx5 (GNSS; PolaRx5), Trimble NETRS (GPS only; NETRS), and Topcon NET-G3A (GPS-only; NET-G3A). Site EBMD, operated by the East Bay Municipal Utility District, has a NET-3GA receiver and Leica AR10 antenna. The telemetry types listed are CM = Cell Modem, R = Radio, Int = Internet, VSAT = Satellite, T1 = Private T1 line. Telemetry often includes a radio hop from the GNSS site to the seismic vault, indicated by an initial R. All (except EBMD) are equipped with Ashtech or Topcon choke ring antennas (CR). Partner-operated sites will not be maintained under this proposal, but are included for informational purposes.

2.2 *GPS data for Real-time Earthquake Information*

Following a major earthquake, the mobilization of local, state, and federal disaster operations can be greatly enhanced by dependable, near real-time estimates of location, magnitude, mechanism, and extent of strong ground shaking. This information can be used to rapidly identify endangered communities, to evaluate the impact on lifelines, and to provide input for damage and loss estimation. In particular, earthquake early warning (EEW) has great potential to improve earthquake response by providing seconds-to-tens of seconds of warning to some locations before strong shaking arrives. Rapid estimation of magnitudes for large events from seismic data alone is known to fail for great earthquakes, where a point source approximation becomes inadequate [*Hoshiba et al.*, 2011]. While real-time GNSS suffers from poor resolution for small events (M_w<6) and requires additional time to wait for static displacements, which arrive with the S-wave, it has demonstrated great potential to reliably determine large magnitudes through finite fault models [*Crowell et al.*, 2009; *Colombelli et al.*, 2013].

In 2011, UC Berkeley, Caltech and the University of Washington received support from the Gordon and Betty Moore foundation to develop the USGS-funded California ShakeAlert

program into a West-Coast-wide prototype system that delivers warnings to industry partners. The Moore foundation grant also funded research and development to improve the system's performance. At the BSL, we have concentrated on improving the performance of EEW for very large earthquakes using information from GNSS. This included establishing real-time processing of incoming BARD GNSS data streams using TrackRT, method development to estimate earthquake magnitude and fault length in real-time [*Colombelli et al.*, 2013], and development of the Geodetic Alarm System (G-larmS) framework to implement real-time monitoring and warning [*Grapenthin et al.*, 2014].

All BARD sites provide real-time data for EEW purposes. Several groups now routinely produce real-time displacements using a variety of software [*Crowell et al.*, 2009; e.g. *Grapenthin et al.*, 2014; *Langbein et al.*, 2014]. Recent upgrades to Septentrio receivers at many BARD sites include onboard precise point positioning (PPP), allowing the potential to broadcast PPP solutions in real-time in the future without the use of additional processing. Real-time streaming of all data from BARD stations was made possible by hardware upgrades from the American Recovery and Reinvestment Act (ARRA), and was implemented immediately thereafter. Multiple groups involved in testing and developing geodetic EEW pick up these streams, including the USGS, Scripps Institute of Oceanography, and Central Washington University. It has the potential to further be improved by combining real-time GNSS data with seismic data. The high number of BARD sites co-located with broadband and seismometers (Figure 2) in the BDSN network means that we are already set to make both data streams available for combination and can provide a test bed for method development.

While real-time processing of GNSS data is capable of providing measurements of displacement within seconds of its occurrence, post-processing provides results with lower noise levels, leading to better precision. This in turn leads to better estimates of the finite fault plane, which when used with ShakeMap, provides more accurate shaking estimates than a point source model. Rapid post-processing (RPP) techniques can be used to estimate static offsets from moderate to large earthquakes, which will constrain a non-linear search for fault plane parameters. RPP requires waiting 1-2 minutes after the earthquake for data to accumulate, but displacement time series can then be generated within 5 minutes using the software Track, developed at MIT. From these, full fault plane determination can be performed within another 5 minutes. While real-time processing techniques are critical for using GNSS data for EEW, rapid post-processing provides higher precision in the static offset measurement. This allows GNSS data to be used for smaller earthquakes and still finishes within a time frame appropriate for ShakeMap. Nonetheless, real-time streaming of GNSS data is still critical for RPP, as it must be available as soon as an event occurs.

The need for real-time GNSS in earthquake early warning was demonstrated earlier this year by the M 7.1 Ridgecrest earthquake. ShakeAlert, which does not yet include a GNSS component, reached its final magnitude estimate of 6.3 around 20 seconds after the origin time. By contrast, the geodetic earthquake early warning algorithm G-larmS, running on a replay of real-time precise point positioning (PPP) data from the Ridgecrest event, reaches a magnitude estimate of 6.7 at 19 seconds past the origin time, which increased to 7.0 at 25 seconds and then held steady (**Figure 1**). This is much closer to the true magnitude of 7.1. A more accurate magnitude estimate in the operational ShakeAlert system would have led to more accurate predictions of ground shaking, especially in the Los Angeles region. Los Angeles did not experience shaking from the Ridgecrest earthquake until approximately 48 seconds past the origin time, more than 20 seconds after G-larmS had estimated a magnitude of 7.0, significantly higher than the 6.3

estimated by ShakeAlert. While this earthquake occurred outside of the BARD network, it demonstrates the need for GNSS for earthquake early warning.

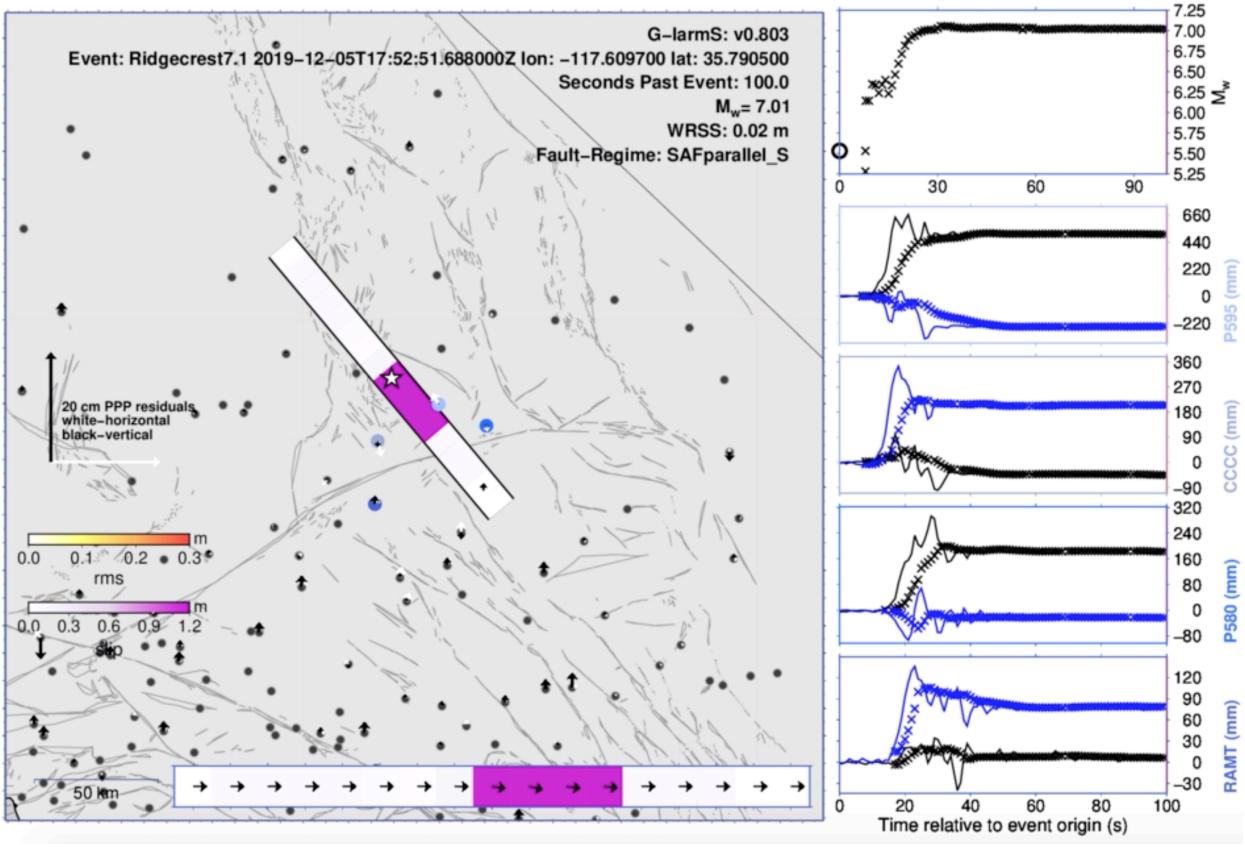

Figure 1. Output of G-larmS for the Ridgecrest earthquake. Vectors shown are residuals between observed and modeled GNSS offsets. The map and fault schematic at the bottom of the figure illustrate the final finite fault model. The 4 sites highlighted in various shades of blue correspond to the timeseries on the right, with the color of the site on the map corresponding to the color of the station name. In the timeseries plots, the line shows the GNSS displacement record, and the x symbols indicate the G-larmS estimated offsets at these sites as a function of time past the origin time. The plot in the upper right corner shows the magnitude estimate as a function of time past the origin time.

2.3 *Data Management Practices*

Continuous data archival

All data collected from BARD/BSL stations are publicly available at the NCEDC (http://www.ncedc.org, ftp://www.ncedc.org/pub/gps), both as raw data and converted into RINEX format. High-rate (1 Hz) data are additionally downsampled to 15-sec sampling and archived in RINEX format to facilitate low-rate processing. The NCEDC also archives raw and RINEX data from 8 continuous stations operated by the USGS, Menlo Park, on a daily basis, as well as from those that are telemetered directly to the BSL though operated by another agency (UCD1 & EBMD).

We participate in the UNAVCO-sponsored GPS Seamless Archive Center (GSAC) project, which provides access to survey-mode and continuous GPS data distributed over many archives.

We have been in contact with personnel from UNAVCO regarding GSAC2.0 and intend to pursue federated status when it is released. This will allow easier web access from central portal sites to NCEDC GPS data. Data from five of our sites (HOPB, MHCB, CMBB, OHLN, YBHB) are sent to the National Geodetic Survey (NGS) in the framework of the CORS (Continuously Operating Reference Stations) project (http://www.ngs.noaa.gov/CORS/). The data from these five sites are also distributed to the public through the CORS ftp site.

Campaign data archival

As part of the activities funded by the USGS through the BARD network, the NCEDC is the principal archive of the 7000+ survey-mode occupations collected by the USGS since 1992. The initial dataset archived was the survey-mode GPS data collected by the USGS Menlo Park for northern California and other locations. Significant quality control efforts were implemented by the NCEDC to ensure that the raw data, scanned site log sheets, and RINEX data are archived for each survey. All of the USGS-MP GPS data transferred to the NCEDC have been archived and are available for distribution through the NCEDC ftp server (ftp://www.ncedc.org/pub/gps/survey/).

Real-time streaming

Our data dissemination program includes real time streaming from all BARD/BSL sites in both RTCM3.0 and BINEX formats. The BSL is also the public portal for real-time streams from the 8 continuous GPS stations operated by the USGS, Menlo Park. The NTRIP-caster we are using to stream the BARD and USGS data is also being used to relay RT17 (Trimble proprietary format) data from stations in the Parkfield area to UC San Diego. Access to the real-time data streams requires an account, though anyone may request and receive an account. Details are on the streaming webpage (http://seismo.berkeley.edu/bard/realtime).

Metadata

The BARD website houses station information and data quality information, as well as providing links to full station metadata, housed at the NCEDC. The BARD website (http://seismo.berkeley.edu/bard) includes individual station pages with basic information and links to daily time series figures and results. We perform basic data quality evaluation for BARD stations, including keeping track of data completeness (number of recorded epochs per number expected), the number of cycle slips detected and the RMS of the estimated multipath parameters for L1 and L2. All are obtained from the program TEQC, developed by UNAVCO. These quantities are updated daily and posted in graphical form to each station's individual webpage.

The authoritative source for BARD station metadata is in IGS format log files, housed at the NCEDC, which are up-to-date and compliant with the most current IGS recommended format. Data quality plots are updated daily, while other information is updated in concert with the log files.

Positions and Time Series

The Berkeley Sesimo Lab is no longer funded to go in-house processing of daily position timeseries. However, daily position time series for BARD stations are processed and made available by the USGS (https://earthquake.usgs.gov/monitoring/gps) and the University of Nevada – Reno geodetic laboratory (http://geodesy.unr.edu/PlugNPlayPortal.php). BSL continues to provide "real-time" 1 Hz baseline timeseries using TrackRT for the BARD network; solutions are available via NTRIP Caster and RabbitMQ broker

(https://igs.bkg.bund.de/ntrip/caster). The real-time positions are used by external researchers for a variety of applications and for geodetic earthquake early warning. An example is Berkeley's own G-larmS project. The new Septentrio receivers have onboard Precise Point Positioning (PPP) capabilities, allowing our real-time stream to soon include positions in addition to baselines.

Publications using data from the project

Most of these studies use BARD data indirectly by using processed position time series from BARD sites obtained from an external processing center.

Chaussard, E., R. Bürgmann, H. Fattahi, C. W. Johnson, R. Nadeau, T. Taira, and I. Johanson (2015), Interseismic coupling and refined earthquake potential on the Hayward-Calaveras fault zone *J. Geophys. Res.*, 120, doi:10.1002/2015JB012230.

Field, E. H., Biasi, G. P., Bird, P., Dawson, T. E., Felzer, K. R., Jackson, D. D. et al. (2015). Long-Term Time-Dependent Probabilities for the Third Uniform California Earthquake Rupture Forecast (UCERF3). *Bulletin of the Seismological Society of America, 105* (2A), 511-543.

Field, E.H., Biasi, G.P., Bird, P., Dawson, T.E., Felzer, K.R., Jackson, D.D., Johnson, K.M., Jordan, T.H., Madden, C., Michael, A.J., Milner, K.R., Page, M.T., Parsons, T., Powers, P.M., Shaw, B.E., Thatcher, W.R., Weldon, R.J., II, and Zeng, Y. (2013), Uniform California earthquake rupture forecast, version 3 (UCERF3)—The time-independent model: U.S. Geological Survey Open-File Report 2013–1165, 97 p., California Geological Survey Special Report 228, and Southern California Earthquake Center Publication 1792, http://pubs.usgs.gov/of/2013/1165/.

Floyd, M. A., et al. (2016), Spatial variations in fault friction controlled by lithology evidenced from the 2014 South Napa earthquake, *Geophys. Res. Lett*., 43, doi:10.1002/2016GL069428.

Hammond, W. C., Burgette, R. J., Johnson, K. M., & Blewitt, G. (2018). Uplift of the Western Transverse Ranges and Ventura Area of Southern California: A Four-Technique Geodetic Study Combining GPS, InSAR, Leveling, and Tide Gauges. *Journal of Geophysical Research: Solid Earth*, *123*(1), 836-858.

Herring, T. A., Melbourne, T. I., Murray, M. H., Floyd, M. A., Szeliga, W. M., King, R. W., Phillips, D. A., Puskas, C. M., Santillan, M., and Wang, L. (2016), Plate Boundary Observatory and related networks: GPS data analysis methods and geodetic products, *Rev. Geophys.*, 54, 759– 808, doi:10.1002/2016RG000529.

Huang, M.-H., R. Bürgmann, and F. Pollitz (2016), Lithospheric rheology constrained from twenty-five years of postseismic deformation following the 1989 Mw 6.9 Loma Prieta earthquake, *Earth Planet. Sci. Lett.,* 435, 147-158, doi:10.1016/j.epsl.2015.12.018. 191.

Johnson, C. W., Y. Fu, and R. Bürgmann (2017), Stress models of the annual hydrospheric, atmospheric, thermal, and tidal loading cycles on California faults: Perturbation of background stress and changes in seismicity, *J. Geophys. Res. Solid Earth*, 122, doi:10.1002/2017JB014778.

Johnson, C. W., Y. Fu, and R. Bürgmann (2017), Seasonal water storage, stress modulation and California seismicity, *Science*, 356(6343), 1161-1164, doi:10.1126/science.aak9547.

Langbein, J., J. R. Evans, F. Blume, and I. A. Johanson (2014), Response of Global Navigation Satellite System receivers to known shaking between 0.2 and 20 Hertz, *U. S. Geological Survey Open-File Rep. 2013-1308*, doi:10.3133/ofr20131308.

Materna, K., N. Bartlow, A. Wech, C. Williams, and R. Bürgmann (2019), Dynamically Triggered Changes of Plate Interface Coupling in Southern Cascadia, *Geophys. Res. Lett.,* 46, doi:10.1029/2019GL084395.

Materna, K., and R. Bürgmann (2016), Contrasts in compliant fault zone properties inferred from geodetic measurements in the San Francisco Bay area, *J. Geophys. Res.- Solid Earth*, 121, doi:10.1002/2016JB013243.

Polcari, M., Palano, M., Fernández, J., Samsonov, S. V., Stramondo, S., and S. Zerbini (2016). 3D displacement field retrieved by integrating Sentinel-1 InSAR and GPS data: the 2014 South Napa earthquake. *European journal of remote sensing*, *49*(1), 1-13.

Rousset, B., R. Bürgmann, and M. Campillo (2018), Slow slip events in the roots of the San Andreas fault, *Sci. Adv., 5*(2), doi:10.1126/sciadv.aav3274.

Shirzaei, M., and R. Bürgmann (2018), Global climate change and local land subsidence exacerbate inundation risk to the San Francisco Bay Area, Sci. Adv., 4(3), doi:10.1126/sciadv.aap9234.

Turner, R. C., M. Shirzaei, R. M. Nadeau, and R. Bürgmann (2015), Slow and Go: Pulsing Slip Rates on the Creeping Section of the San Andreas Fault, *J. Geophys. Res*., 120, doi:10.1002/2015JB011998.

Xu, W., Wu, S., Materna, K., Nadeau, R., Floyd, M., Funning, G., Chaussard, E., Johnson, C., Murray, J., Ding, X., and R. Bürgmann (2018), Interseismic ground deformation and fault slip rates in the greater San Francisco Bay Area from two decades of space geodetic data, *J. Geophys. Res. Solid Earth*, 123, doi:10.1029/2018JB016004.

Zeng, Y., and Shen, Z.-K. (2016). A Fault-Based Model for Crustal Deformation, Fault Slip Rates, and Off-Fault Strain Rate in California. *Bulletin of the Seismological Society of America, 106*(2), 766–784.

References

Borsa, A. A., Agnew, D. C., & Cayan, D. R. (2014). Ongoing drought-induced uplift in the western United States. Science, 345(6204), 1587-1590.

Bürgmann, R., Hilley, G., Ferretti, A., & Novali, F. (2006). Resolving vertical tectonics in the San Francisco Bay Area from permanent scatterer InSAR and GPS analysis. *Geology, 34*(3), 221-224.

Bürgmann, R., P. Segall, M. Lisowski, and J. Svarc (1997), Postseismic strain following the 1989 Loma Prieta earthquake from GPS and leveling measurements, *J. Geophys. Res.*, 102, 4933–4955.

Chaussard, E., Bürgmann, R., Fattahi, H., Nadeau, R. M., Taira, T., Johnson, C. W., & Johanson, I. (2015). Potential for larger earthquakes in the East San Francisco Bay Area due to the direct connection between the Hayward and Calaveras Faults. *Geophysical Research Letters*, *42*(8), 2734-2741.

Colombelli, S., R. M. Allen, and A. Zollo (2013), Application of real-time GPS to earthquake early warning in subduction and strike-slip environments, *J. Geophys. Res.*, n/a–n/a, doi:10.1002/jgrb.50242.

Crowell, B. W., Y. Bock, and M. B. Squibb (2009), Demonstration of Earthquake Early Warning Using Total Displacement Waveforms from Real-time GPS Networks, *Seismological Research Letters*, *80*(5), 772–782, doi:10.1785/gssrl.80.5.772.

Detweiler, S.T., and Wein, A.M., eds. (2017) The HayWired earthquake scenario—Earthquake hazards (ver. 1.2, December 2018): U.S. Geological Survey Scientific Investigations Report 2017–5013–A–H, 126 p., https://doi.org/10.3133/sir20175013v1.

Field, E. H., Biasi, G. P., Bird, P., Dawson, T. E., Felzer, K. R., Jackson, D. D. et al. (2015). Long-Term Time-Dependent Probabilities for the Third Uniform California Earthquake Rupture Forecast (UCERF3). *Bulletin of the Seismological Society of America, 105* (2A), 511-543.

Field, E.H., Biasi, G.P., Bird, P., Dawson, T.E., Felzer, K.R., Jackson, D.D., Johnson, K.M., Jordan, T.H., Madden, C., Michael, A.J., Milner, K.R., Page, M.T., Parsons, T., Powers, P.M., Shaw, B.E., Thatcher, W.R., Weldon, R.J., II, and Zeng, Y. (2013), Uniform California earthquake rupture forecast, version 3 (UCERF3)—The time-independent model: U.S. Geological Survey Open-File Report 2013–1165, 97 p., California Geological Survey Special Report 228, and Southern California Earthquake Center Publication 1792, http://pubs.usgs.gov/of/2013/1165/.

Grapenthin, R., Johanson, I. A., & Allen, R. M. (2014). Operational real-time GPS-enhanced earthquake early warning. *Journal of Geophysical Research: Solid Earth*, *119*(10), 7944-7965.

Gwyther, R. L., C. H. Thurber, M. T. Gladwin, and M. Mee (2000), Seismic and aseismic observations of the 12th August 1998 San Juan Bautista, California M5.3 earthquake, *3rd San Andreas Fault Conference*, 209–213.

Hoshiba, M., K. Iwakiri, N. Hayashimoto, T. Shimoyama, K. Hirano, Y. Yamada, Y. Ishigaki, and H. Kikuta (2011), Outline of the 2011 off the Pacific coast of Tohoku Earthquake (Mw9.0)― Earthquake Early Warning and observed seismic intensity―, *Earth Planets Space*, *63*(7), 547–551, doi:10.5047/eps.2011.05.031.

Huang, M.-H., R. Bürgmann, and F. Pollitz (2016), Lithospheric rheology constrained from twenty-five years of postseismic deformation following the 1989 Mw 6.9 Loma Prieta earthquake, *Earth Planet. Sci. Lett.*, 435, 147-158, doi:10.1016/j.epsl.2015.12.018. 191.

Lienkaemper, J. J., J. Galehouse, and R. Simpson (1997), Creep Response of the Hayward Fault to Stress Changes Caused by the Loma Prieta Earthquake, *Science*, *276*(5321), 2014–2016

Linde, A. T., M. Gladwin, M. Johnston, R. Gwyther, and R. Bilham (1996), A slow earthquake sequence on the San Andreas fault, *Nature*, *383*(6595), 65–68.

Materna, K., Bartlow, N., Wech, A., Williams, C., and Bürgmann, R. (2019). Dynamically triggered changes of plate interface coupling in Southern Cascadia. *Geophysical Research Letters*, 46, 12890– 12899. https://doi.org/10.1029/2019GL084395

McFarland, F. S., J. J. Lienkaemper, and S. J. Caskey (2013), Data from Theodolite Measurements of Creep Rates on San Francisco Bay Region Faults, California, 1979-2012, v. 1.4, *U. S. Geological Survey Open-File Rep. 2009-1119*, 1–18.

Miller, M. M., T. Melbourne, D. J. Johnson, and W. Q. Sumner (2002), Periodic slow earthquakes from the Cascadia subduction zone, *Science*, *295*(5564), 2423–2423.

Rousset, B., R. Bürgmann, and M. Campillo (2018), Slow slip events in the roots of the San Andreas fault, *Sci. Adv., 5*(2), doi:10.1126/sciadv.aav3274.

Segall, P., R. Bürgmann, and M. Matthews (2000), Time-dependent triggered afterslip following the 1989 Loma Prieta earthquake, *J. Geophys. Res.*, *105*(B3), 5615–5634, doi:10.1029/1999JB900352.

Thatcher, W. (1983), Nonlinear strain buildup and the earthquake cycle on the San Andreas Fault, *Journal of Geophysical Research*, *88*(B7), 5893, doi:10.1029/JB088iB07p05893.

Toppozada, T. R., & Borchardt, G. (1998). Re-evaluation of the 1836 "Hayward fault" and the 1838 San Andreas fault earthquakes. *Bulletin of the Seismological Society of America*, *88*(1), 140-159.

Uhrhammer, R., L. Gee, and M. Murray (1999), The Mw 5.1 San Juan Bautista, California earthquake of 12 August 1998, *Seismological Research Letters*.

Xu, W., Wu, S., Materna, K., Nadeau, R., Floyd, M., Funning, G., et al. (2018). Interseismic ground deformation and fault slip rates in the greater San Francisco Bay Area from two decades of space geodetic data. Journal of Geophysical Research: Solid Earth, 123, 8095– 8109. https://doi.org/10.1029/2018JB016004

Zeng, Y., and Shen, Z.-K. (2016). A Fault-Based Model for Crustal Deformation, Fault Slip Rates, and Off-Fault Strain Rate in California. *Bulletin of the Seismological Society of America, 106*(2), 766–784.